



ADAPTIVE STRUCTURES FOR LARGE PRECISION ANTENNAS†

BRIJ N. AGRAWAL and HYOCHOONG BANG

Naval Postgraduate School, Department of Aeronautics and Astronautics, Monterey, CA 93943, U.S.A.

(Received 24 May 1995)

Abstract—Optimal controller design approach for high precision pointing maneuver of flexible spacecraft by using adaptive structures is investigated in this paper. A parameter optimization technique is used to find out controller parameters minimizing a desired objective function which represents pointing performance of a flexible space structure. Multi-input and multi-output configuration used in this study also provides insight on the effectiveness of actuator location for improved performance. Copyright © 1996 Elsevier Science Ltd

1. INTRODUCTION

Various control approaches have emerged for flexible spacecraft maneuver and vibration control tasks [1,2]. The inherent flexibility in the spacecraft makes control law design work very challenging. This is quite true, especially for the case where the desired maneuver accuracy is so high that the interaction between the structure and controllers should be fully taken into account.

Active control design using adaptive structures due to its inherent advantages has received significant attention. One of the promising approaches is a feedback law based upon second order compensators which are driven by physical sensor outputs. For the case where position sensor outputs are available, this approach is called Positive Position Feedback (PPF). The PPF design method has been tested in a series of previous studies in conjunction with adaptive structures [3,4]. It is considered as being useful for collocated sensor/actuator systems even in the presence of actuator dynamics which may cause a potential stability problem. The PPF design, however, has not been fully characterized in terms of robustness as well as performance criterion.

In this study, we investigate the PPF approach from performance perspective. This study is motivated by a control goal of minimizing tip displacement and rotation of a flexible spacecraft structure. In other words, the PPF performance is optimized for active vibration control of a flexible structure. The original PPF subject to a stability constraint is enhanced by optimizing design parameters associated with the PPF.

Compensator design based upon position output only has some inherent advantages, due to the simple structure of the compensator, for which, the main role is to estimate rate information using the position sensor output. A difficult question on the PPF compensator design is how to select a stabilizing set of feedback gains under the influence of multi modes of vibration. The routine application of root locus analysis has limitations, especially for high order multi-input systems. The spectral distribution of the system natural frequencies influences the closed loop system performance in an undesirable manner; this is true in conjunction with arbitrary selected feedback gains.

The selection of PPF gains is dictated by a stability criterion which is in the form of positive definiteness of a matrix consisting of feedback gains and system parameters [3,4]. It is not, however a straightforward procedure to rely on such a single criterion to find a desirable set of feedback gains. The stability criterion is a rather passive approach in the sense that one can have only stable regions of feedback gains. No particular insight on the efficiency of the feedback gains is provided by the stability criterion alone.

As an extension to the conventional PPF design approach, we seek to set up another criterion, i.e. a cost function to be minimized by feedback gains which are subject to the stability criterion at the same time. The cost function is usually selected in an effort to provide more efficiency of the control action to the system. Also, some of the robustness measures can be combined in the cost function for robustness of the closed loop system. By introducing the cost function and associated stability constraints, we can find the feedback gains which achieve the design objective in a more systematical way.

†Paper IAF 94.1.4.202, presented at the 45th International Astronautical Congress, Jerusalem, Israel, 9-14 October 1994.

2. MODEL EQUATION AND PPF COMPENSATOR

For a general linearized second order system, the governing equations of motion are given by

$$M\ddot{\mathbf{q}} + K\mathbf{q} = a_1Fu \tag{1}$$

where \mathbf{q} is the generalized coordinate vector, a_1 is a constant related to actuator sensitivity, and M, K are the mass and stiffness matrices, respectively. The above equation can be rewritten in the modal coordinate form including modal damping as follows

$$\ddot{\eta} + D\dot{\eta} + \Omega\eta = a_1\bar{F}u \tag{2}$$

where η is the modal coordinate vector defined by $\mathbf{q} = \Phi\eta$, $\bar{F} = \Phi^T F$ is a modal control distribution matrix, and D is the modal damping matrix. Next, the compensator equation can also be written in the modal coordinate form as follows

$$\ddot{\xi} + D_f\dot{\xi} + \Omega_f\xi = a_2\Omega_f\mathbf{y} \tag{3}$$

where \mathbf{y} is a measurement vector from the sensor and a_2 is a constant representing sensor sensitivity. As a special case of collocated sensor/actuator system, the measurement vector \mathbf{y} is given by [4, 6]

$$\mathbf{y} = F^T\mathbf{q}.$$

The above equation is true for a position sensing device such as piezoceramic sensor used in this study. Then eqn (3) can be rewritten as

$$\ddot{\xi} + D_f\dot{\xi} + \Omega_f\xi = a_2\Omega_f E F^T \Phi \eta \tag{4}$$

where E is a special constant matrix introduced to diagonalize a feedback gain matrix even in the case of single sensor/actuator system and multi-mode compensators. Now, by choosing an appropriate E and the control input u in the form of position feedback from compensator output, we arrive at the following set of system and compensator equations [3,4]

$$\begin{aligned} \ddot{\eta} + D\dot{\eta} + \Omega\eta &= a_1 C^T G \xi \\ \ddot{\xi} + D_f\dot{\xi} + \Omega_f\xi &= a_2 \Omega_f C \eta \end{aligned} \tag{5}$$

The stability condition for the two combined systems can be written as

$$\Omega - a_1 a_2 C^T G C > 0 \tag{6}$$

i.e. the matrix should be positive definite. Note that feedback gain matrix G consists of each feedback gain which is associated with each flexible mode. It also should be noticed that the stability criterion in eqn (6) does not depend on the structural properties of the compensator. For a single mode control with single compensator, it can easily be shown that the controller efficiency is maximized when the compensator and system natural frequencies match together. This can be proven by using a frequency response function and phase relationship between compensator input governed by system dynamics and compensator output.

3. OPTIMIZATION OF FEEDBACK GAINS

The PPF design in the previous part can be characterized by a stabilizing feedback gain space as prescribed in eqn (6). The direct selection of feedback gains is not, however, a simple task due to the implicit form of the inequality constraint equation. Small gains are feasible choices since a_1 and a_2 are usually in small orders of magnitude. However, especially for the multi-mode case, a more systematic approach is required for better performance of the compensator.

Motivated by general optimization of a Linear Quadratic Regulator (LQR) cost function, we suggest the following cost function to be minimized by the feedback gains being subject to the constraint equation, eqn (6).

$$J(\mathbf{p}) = \frac{1}{2} \int_0^{\infty} (\mathbf{x}^T Q_c \mathbf{x} + \mathbf{u}^T Q_u \mathbf{u}) dt \tag{7}$$

where $\mathbf{p} \equiv [p_1, p_2, \dots, p_n]$ is a vector of design parameter consisting of feedback gains and $\mathbf{x} = [\eta, \dot{\eta}, \xi, \dot{\xi}]^T$ is a state vector for eqn (5) in a first order state space form. In other words, eqn (5) can be rewritten as

$$\frac{d}{dt} \begin{Bmatrix} \eta \\ \dot{\eta} \\ \xi \\ \dot{\xi} \end{Bmatrix} = \begin{bmatrix} 0 & I & 0 & 0 \\ -\Omega & -D & a_1 C^T G & 0 \\ 0 & 0 & 0 & I \\ a_2 C_f C & 0 & -\Omega_f & -D_f \end{bmatrix} \begin{Bmatrix} \eta \\ \dot{\eta} \\ \xi \\ \dot{\xi} \end{Bmatrix} \tag{8}$$

The above equation, for notational simplicity, is written as

$$\dot{\mathbf{x}} = \bar{A}\mathbf{x}, \text{ for } \mathbf{x}(0) \tag{9}$$

where $\bar{A} = A - BG$, and $\mathbf{u} = -G\mathbf{x}$. Using the above equation, the cost function defined in eqn (7) becomes

$$J(\mathbf{p}) = \frac{1}{2} \mathbf{x}(0)^T [P + P_u] \mathbf{x}(0) \tag{10}$$

where

$$P_s = \int_0^{\infty} e^{\bar{A}^T t} Q_c e^{\bar{A} t} dt, \quad P_u = \int_0^{\infty} e^{\bar{A}^T t} G^T Q G e^{\bar{A} t} dt$$

or

$$J(\mathbf{p}) = \frac{1}{2} \text{trace}[P_s X(0) + P_u X(0)], \quad X(0) = \mathbf{x}(0)\mathbf{x}(0)^T.$$

Hence, our optimization problem can be restated as follows

$$\text{Minimize } J(\mathbf{p}) = \frac{1}{2} \text{trace}(\bar{P}X(0))$$

subject to

$$\Omega - a_1 a_2 C^T g(\mathbf{p}) C > 0 \tag{11}$$

where $\bar{P} = P_s + P_u$. Note that P_s and P_u are positive definite matrices if A is stable and satisfy the following Lyapunov equations[5]

$$\begin{aligned} P_s \bar{A} + \bar{A}^T P_s + Q_s &= 0 \\ P_u \bar{A} + \bar{A}^T P_u + G^T Q_u G &= 0. \end{aligned} \quad (12)$$

For later use in the optimization, the analytical expression for the partial derivative of the cost function J with respect to design parameters is given as follows[5]

$$\frac{\partial J}{\partial p_i} = \text{trace} \left[VP \frac{\partial \bar{A}}{\partial p_i} + V(P_u B - G^T Q_u) \frac{\partial G}{\partial p_i} \right] \quad (13)$$

where V is the solution of the complementary Lyapunov equation

$$V \bar{A}^T + \bar{A} V + X(0) = 0. \quad (14)$$

Therefore, by solving the two Lyapunov equations in eqns (12) and (14), we obtain the cost function and derivative of the cost function with respect to design parameters analytically. Next, we apply an optimization algorithm, so-called Homotopic Nonlinear Programming, by using the information obtained in the above stage.

3.1. Homotopic nonlinear programming

This algorithm is a modification of the original two-stage homotopic nonlinear programming method[7]. The central idea of this algorithm is the use of minimum norm differential correction to iteratively modify the design parameters[7,8]. This algorithm has a close connection with generalized Newton processes for solving a system of underdetermined nonlinear equations. On each iteration, we seek to minimize the norm of s correction vector required to satisfy specified equality constraints. The constraint boundaries are swept in the homotopy process from constraints easily achieved initially to those of the final design. The constraint functions are locally linearized to provide a system of linear algebraic equations to solve for the correction vectors. Locally, only the active constraint set is considered, however, the active set is permitted to change as the iteration progress converges.

The homotopic method is a continuation method using a homotopy parameter which defines a family of sequential nonlinear programming problems. For a given value of the homotopy parameter, the design parameter vector is iteratively updated; upon convergence, the homotopy parameter is updated to transit to the next neighboring set of constraints and objective function. The most recently converged result is used as initial conditions in the iterations to satisfy the new objectives provided by incrementing the homotopy parameter. In the usual successful implementation of this approach, we reach the final desired objective by sweeping the homotopy parameter.

The overall algorithm can be described as follows. First, we seek to find a design parameter vector \mathbf{p} in such a way that

$$\text{Minimize } J(\mathbf{p}), \quad \text{subject to } \Omega - a_1 a_2 C^T G C > 0. \quad (15)$$

First, we define an objective function which is parameterized by a homotopy parameter γ

$$J_0(\gamma) = \gamma J_{\text{goal}} + (1 - \gamma) J(\mathbf{p}_{\text{feasible}}) \quad (16)$$

where γ is called a homotopy parameter sweeping from zero for a trivial case with $J_0 = J(\mathbf{p}_{\text{feasible}})$ to unity with the final desired goal $J_0 = J_{\text{goal}}$. The initial choice of the parameter $\mathbf{p}_{\text{feasible}}$ vector must be found to satisfy the inequality constraints in eqn (15). Sequential programming then consists of sweeping γ with some adaptive increments dictated by convergence progress of updating design parameters \mathbf{p} . Each γ and corresponding $J_0(\gamma)$ defines a portable objective along the way toward J_{goal} . J_{goal} may not be feasible in general, and should be interpreted as "the best one could hope for". When convergence to $J_0(\gamma)$ cannot be achieved for a small tolerance increase in γ , we adopt the solution corresponding to the largest γ for which convergence is achieved as the constrained minimum. We implement this strategy by forming a homotopy map $H(\mathbf{p}(\gamma), \gamma)$

$$H(\mathbf{p}(\gamma), \gamma) \equiv J(\mathbf{p}(\gamma)) - \gamma J_{\text{goal}} - (1 - \gamma) J(\mathbf{p}_{\text{feasible}}) = 0. \quad (17)$$

In order to solve the underdetermined vector function of eqn (17), we linearize eqn (17) with respect to variations in the local $\mathbf{p}(\gamma)$

$$H(\mathbf{p}(\gamma), \gamma) + \tilde{A} \Delta \mathbf{p} = 0 \quad (18)$$

where

$$\tilde{A} = \left[\frac{\partial J}{\partial p_1}, \frac{\partial J}{\partial p_2}, \dots, \frac{\partial J}{\partial p_m} \right].$$

Since eqn (18) is usually underdetermined, we seek a particular solution in such a way that the correction vector $\Delta \mathbf{p}$ minimizes $\frac{1}{2} \Delta \mathbf{p}^T W \Delta \mathbf{p}$ satisfying eqn (18); the result is given by minimum norm differential correction

$$\Delta \mathbf{p} = -W^{-1} \tilde{A}^T (\tilde{A} W^{-1} \tilde{A}^T)^{-1} H(\mathbf{p}(\gamma), \gamma) \quad (19)$$

where W is a positive definite weighting matrix. Once we find $\Delta \mathbf{p}$, we use the differential correction recursion

$$\mathbf{p}_{\text{new}} = \mathbf{p}_{\text{old}} + \Delta \mathbf{p}. \quad (20)$$

The iteration continues until $\Delta \mathbf{p}$ reach certain error tolerance limit. On the convergence of a specific γ , the new objective function is defined by $J_0(\gamma)$ and the same procedure is taken until J_{goal} is achieved.

If the constraint is violated during iterations, the design parameters \mathbf{p} should be reset to satisfy the stability constraint equation. Unless the design parameters are updated on the violation of con-

straints, the closed loop system \bar{A} becomes unstable and the Lyapunov solution may produce ill conditioned or non-positive definite matrices. The constraint violation update algorithm is discussed in the next section.

3.2. Active constraint sets

The stability condition, as shown earlier, is expressed in the form of positive definiteness of a matrix as follows

$$S \equiv \Omega - a_1 a_2 C^T G C > 0.$$

This means that the eigenvalues of S are all positive

$$\lambda_i \phi_i = S \phi_i, \quad \lambda_i > 0, \quad \text{for all } i. \quad (21)$$

It is obvious that the eigenvalues of S are real, since S is a symmetric matrix. For stability margin of S , we introduce a set of constraint boundaries corresponding to each eigenvalue of S as follows

$$\lambda_i \geq \lambda_i^c, \quad \text{for all } i. \quad (22)$$

The above constraints represent restatement of eqn (6) in the form of a set of scalar inequality constraints. The constraint boundaries λ_i^c are prescribed to provide enough stability margin. During the successive sequential programming stage, the stability condition is monitored to find a stabilizing set of feedback gains. If any of the constraints is violated, then the design parameters are updated so that the corresponding constraint set becomes an active set on the prescribed boundary.

When there are m constraint violations during iteration in such a way that

$$\lambda_j < \lambda_j^c, \quad \text{for } j = 1, \dots, m \quad (23)$$

first we form a set of nonlinear equations

$$H_c \equiv \begin{bmatrix} \lambda_1 - \lambda_1^c \\ \lambda_2 - \lambda_2^c \\ \vdots \\ \lambda_m - \lambda_m^c \end{bmatrix} = 0. \quad (24)$$

In order to solve the above set of nonlinear algebraic equations, we take a similar approach as for solving the objective function equations. Next, we linearize the nonlinear equations with respect to the feedback gains and violated constraints

$$H_c + \tilde{L} \Delta \mathbf{p} = 0 \quad (25)$$

where

$$\tilde{L} \equiv \left[\frac{\partial H_c}{\partial p_1}, \frac{\partial H_c}{\partial p_c}, \dots, \frac{\partial H_c}{\partial p_m} \right].$$

The partial derivative $\partial H_c / \partial p_i$ can be obtained analytically by using a commonly known eigenvalue

sensitivity relationship. The eigenvalue sensitivity equation is given by

$$\frac{\partial \lambda_i}{\partial p_k} = \psi_i^T \frac{\partial S}{\partial p_k} \phi_i \quad (26)$$

where ψ_i is an eigenvector obtained by

$$\lambda_i \psi_i = S^T \psi_i. \quad (27)$$

On the other hand, the above set of equations in eqn (25) is usually underdetermined, therefore, can be represented by a minimum norm solution

$$\Delta \mathbf{p} = -W^{-1} \tilde{L}^T (\tilde{L} W^{-1} \tilde{L}^T)^{-1} H_c.$$

Once the differential correction $\Delta \mathbf{p}$ is obtained we update the design parameters as follows

$$\mathbf{p}_{\text{new}} = \mathbf{p}_{\text{old}} + \Delta \mathbf{p}. \quad (28)$$

The constraint update loop should be nested inside the main loop for updating design parameters along with the homotopy parameter (γ). Once the constraint is violated the design parameters are updated to satisfy the constraint equation, eqn (24), then on the next stage with new homotopy parameter γ , the design parameters are set free to change. If the constraints keep violated on the new objective function, the most recent set of design parameters which satisfy the prescribed constraint boundaries is taken as a sub-optimal solution[7].

4. APPLICATION

An application has been made to demonstrate the technique developed up to now. The system used is a spacecraft model which has been used for vibration control experiment[9]. The schematic representation of the model is presented in Figs 1 and 2. As can be seen, it consists of two elastic structures connected in orthogonal configuration. It represents space structures such as antennas or reflectors. Three sets of sensors and actuators are located on the positions indicated in Fig. 1. The deformed configuration and notations are provided in Fig. 2.

Previous studies using the same model have been conducted for experimental verification of PPF and further enhancement of the original PPF approach[9]. The main objective of this study is to design compensators with optimized feedback gains. As a particular case, it is required to minimize the deflection and rotation at the tip of the second structure. This is a rather realistic goal in the sense that the tip movement represents degradation of antenna pointing accuracy.

In order to implement the optimization algorithm, first we seek to set up the cost function. The position vector locating the infinitesimal element of the first and second elastic domain is represented using the notations in Fig. 2 as follows

$$R_1 = y_1 \hat{n}_1 + x_1 \hat{n}_2, \quad R_2 = y_2 \hat{b}_1 + x_2 \hat{b}_2. \quad (29)$$

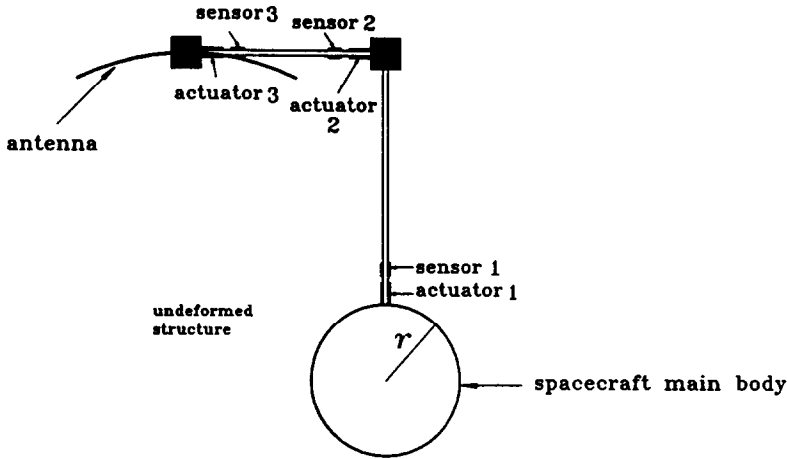


Fig. 1. Undeformed configuration of flexible space structure model.

The body fixed coordinate system (\hat{b}_1, \hat{b}_2) is related to the inertially fixed coordinate system (\hat{n}_1, \hat{n}_2) as follows

$$\begin{Bmatrix} \hat{b}_1 \\ \hat{b}_2 \end{Bmatrix} = \begin{bmatrix} \cos \alpha & -\sin \alpha \\ -\sin \alpha & -\cos \alpha \end{bmatrix} \begin{Bmatrix} \hat{n}_1 \\ \hat{n}_2 \end{Bmatrix}$$

where $\alpha = \partial y_1 / \partial x|_1$ is the rotation at the tip of the first structure. Therefore,

$$R_2 = (x_2 \cos \alpha - y_2 \sin \alpha) \hat{n}_1 + (-x_2 \sin \alpha - y_2 \cos \alpha) \hat{n}_2.$$

The tip displacement of the second structure which is the main parameter of concern can be written in terms of the tip position vectors of the first and second structures

$$\begin{aligned} R^t &= R_1^t + R_2^t \\ &= (y_1^t + l_2 \cos \alpha - y_2^t \sin \alpha) \hat{n}_1 \\ &\quad + (l_1 - l_2 \sin \alpha - y_2^t \cos \alpha) \hat{n}_2. \end{aligned} \quad (30)$$

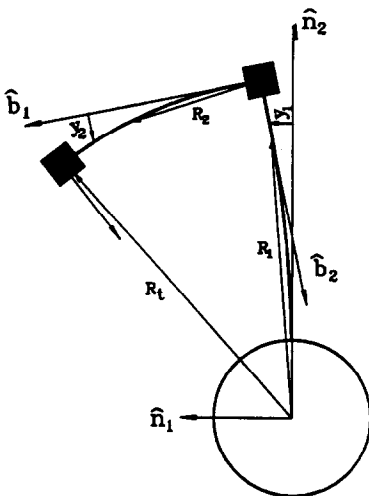


Fig. 2. Deformed configuration and notations.

Assuming small deflection and rotation, the tip position vector can be rewritten as

$$R^t = (y_1^t + l_2) \hat{n}_1 + (l_1 - l_2 \alpha - y_2^t) \hat{n}_2. \quad (31)$$

Introducing the original undeformed tip position vector as

$$R_u^t = l_2 \hat{n}_1 + l_1 \hat{n}_1 \quad (32)$$

we can define an error vector as follows

$$E^t = R^t - R_u^t = y_1^t \hat{n}_1 + (-l_2 \alpha - y_2^t) \hat{n}_2. \quad (33)$$

Furthermore, the total rotational angle at the tip can be written as

$$\Phi = (\alpha + \beta) \hat{n}_3 \quad (34)$$

where $\beta = \partial y_2 / \partial x|_2$ denotes rotation at the tip of the second structure. Based upon the definition of the tip pointing error, the following cost function is suggested for optimization

$$\begin{aligned} J &= \int_0^x [(y_1^t)^2 + w_1(l_2 \alpha + y_2^t)^2 + w_2 \Phi^2 + u^T Q u] dt \\ &= \int_0^x [\zeta_t^T \bar{Q} \zeta_t + u^T Q u] dt \end{aligned} \quad (35)$$

where

$$\bar{Q} = \begin{bmatrix} 1 & 0 & 0 & 0 \\ 0 & w_1 l_2^2 + w_2 & w_1 l_2 & w_2 \\ 0 & w_1 l_2 & w_1 & 0 \\ 0 & w_2 & 0 & w_2 \end{bmatrix}, \quad \zeta_t = \begin{Bmatrix} y_1^t \\ \alpha \\ y_2^t \\ \beta \end{Bmatrix}.$$

On the other hand, a mathematical model of the system is developed using the finite element method. Therefore, the system model can be written in terms of linearized second order vector equations as

$$M \ddot{q} + K q = F u.$$

Table 1. (a) Optimization results with first mode excitation ($w_1 = 100, w_2 = 100$)

	Gains	Actuator 1	Actuator 2	Actuator 3	Cost (J)
Initial	g_1	1.0000×10^2	1.0000×10^2	1.0000×10^2	3.1239×10^5
	g_2	1.0000×10^2	1.0000×10^2	1.0000×10^2	
	g_3	1.0000×10^2	1.0000×10^2	1.0000×10^2	
Optimized $\gamma = 0.9$	g_1	9.2108×10^4	1.5109×10^4	1.0567×10^2	3.1309×10^5
	g_2	8.8999×10^4	1.0013×10^4	1.0515×10^2	
	g_3	3.7144×10^4	4.1053×10^2	1.0188×10^2	

(b) With three modes excitation ($w_1 = 100, w_2 = 100$)

	Gains	Actuator 1	Actuator 2	Actuator 3	Cost (J)
Initial	g_1	1.000×10^2	1.0000×10^2	1.0000×10^2	3.4996×10^5
	g_2	1.0000×10^2	1.0000×10^2	1.0000×10^2	
	g_3	1.0000×10^2	1.0000×10^2	1.0000×10^2	
Optimized $\gamma = 0.9$	g_1	9.0695×10^4	1.5182×10^4	1.0633×10^2	3.5066×10^5
	g_2	9.6529×10^4	1.7370×10^4	1.1196×10^2	
	g_3	5.6419×10^4	6.8916×10^3	2.0002×10^2	

The piezoceramic actuator used in the previous study and in this analysis are known to produce bending moment, when driven by voltage actuation[4,9].

$$M_a = a_1 V_c \quad (36)$$

where V_c is applied voltage, M_a bending moment applied to the beam, and k is a constant which represents actuator characteristics. This relationship in eqn (36) is incorporated into eqn (2) in the form of the input influence matrix (F) and applied inputs (u). The piezoceramic sensor, on the other hand, produces a voltage signal proportional to the strain (or moment) level in the structure, and essentially is dual to the actuator in operational principle[4,9]

$$y = a_2 M(x, t) \quad (37)$$

where M is the bending moment developed in the structure. Therefore, the actuator and sensor with the same operational principle can be described as eqn (4).

For practical reasons, three flexible modes are included in the system model described in modal coordinates. Each actuator plays the role of controlling all three modes, therefore need three sets

of compensators and nine overall. In other words, the feedback gain matrix (G) has the form

$$G = \begin{bmatrix} \bar{G}_1 & & \\ & \bar{G}_2 & \\ & & \bar{G}_3 \end{bmatrix} \quad (38)$$

where each sub-gain matrix (G_i) corresponds to the i th actuator, and can be written as

$$\bar{G}_i = \begin{bmatrix} g_{i1} & & \\ & g_{i2} & \\ & & g_{i3} \end{bmatrix}, \quad i = 1, 2, 3 \quad (39)$$

where each gain (g_{ij}) is associated with the compensator output for the j th mode.

The optimized gains and associated cost function are presented in Tables 1–3. The parameters used in this application are $Q = 10^{-8}$, and three sets of weighting factors (w_1, w_2), i.e. (1) $w_1 = 100, w_2 = 100$, (2) $w_1 = 500, w_2 = 100$, (3) $w_1 = 100, w_2 = 500$, respectively. Tables 1–3 present results with different combinations of w_1 and w_2 . For verification of computer code and the characteristic of PPF, only the first flexible mode is excited first, which is followed by three modes excitation.

Table 2. (a) Optimization results with first mode excitation ($w_1 = 500, w_2 = 100$)

	Gains	Actuator 1	Actuator 2	Actuator 3	Cost (J)
Initial	g_1	1.0000×10^2	1.0000×10^2	1.0000×10^2	6.4476×10^5
	g_2	1.0000×10^2	1.0000×10^2	1.0000×10^2	
	g_3	1.0000×10^2	1.0000×10^2	1.0000×10^2	
Optimized $\gamma = 0.9$	g_1	1.5166×10^5	2.1829×10^4	1.1040×10^2	6.4546×10^5
	g_2	1.6428×10^5	1.1710×10^4	1.1176×10^2	
	g_3	8.5035×10^4	-2.8756×10^3	1.0647×10^2	

(b) With three modes excitation ($w_1 = 500, w_2 = 100$)

	Gains	Actuator 1	Actuator 2	Actuator 3	Cost (J)
Initial	g_1	1.0000×10^2	1.0000×10^2	1.0000×10^2	7.0002×10^5
	g_2	1.0000×10^2	1.0000×10^2	1.0000×10^2	
	g_3	1.0000×10^2	1.0000×10^2	1.0000×10^2	
Optimized $\gamma = 0.9$	g_1	1.4748×10^5	2.1694×10^4	1.1127×10^2	7.0073×10^5
	g_2	1.6946×10^5	2.2177×10^4	1.2016×10^2	
	g_3	1.0588×10^5	6.5468×10^3	2.2375×10^2	

Table 3. (a) Optimization results with first mode excitation ($w_1 = 100, w_2 = 500$)

	Gains	Actuator 1	Actuator 2	Actuator 3	Cost (J)
Initial	g_1	1.0000×10^2	1.0000×10^2	1.0000×10^2	1.2288×10^6
	g_2	1.0000×10^2	1.0000×10^2	1.0000×10^2	
	g_3	1.0000×10^2	1.0000×10^2	1.0000×10^2	
Optimized $\gamma = 0.9$	g_1	2.0822×10^5	2.5027×10^4	1.776×10^2	1.2299×10^5
	g_2	2.5631×10^5	7.0151×10^3	1.1813×10^2	
	g_3	1.5904×10^5	-1.1803×10^4	1.0884×10^2	

(b) With three modes excitation ($w_1 = 100, w_2 = 500$)

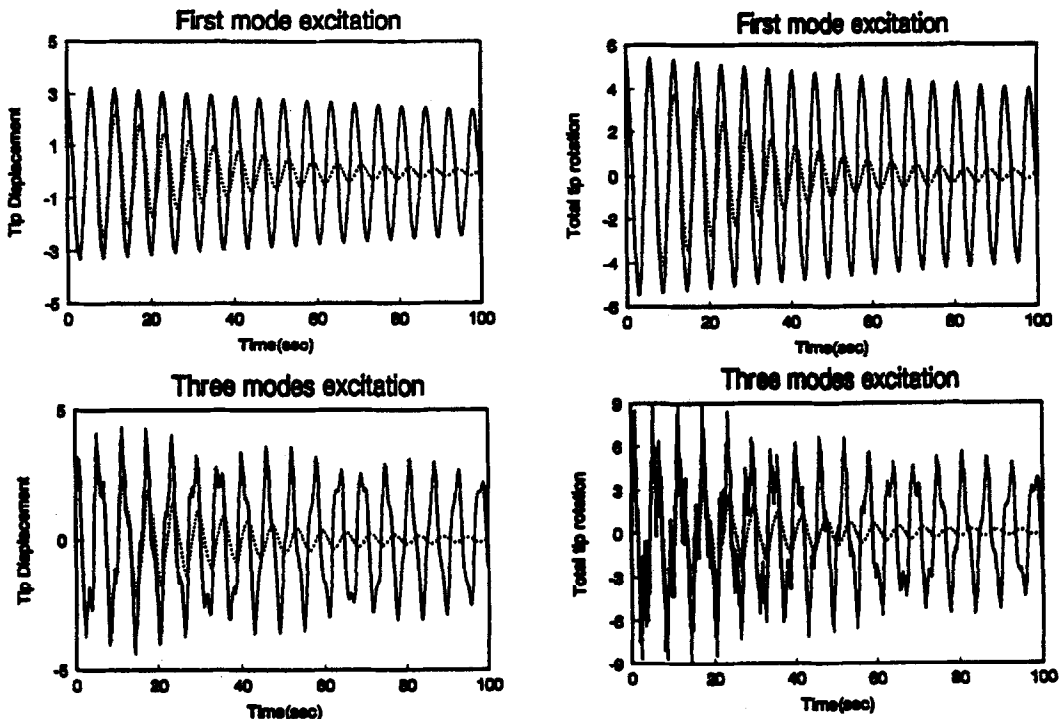
	Gains	Actuator 1	Actuator 2	Actuator 3	Cost (J)
Initial	g_1	1.0000×10^2	1.0000×10^2	1.0000×10^2	1.3989×10^6
	g_2	1.0000×10^2	1.0000×10^2	1.0000×10^2	
	g_3	1.0000×10^2	1.0000×10^2	1.0000×10^2	
Optimized $\gamma = 0.9$	g_1	2.0229×10^5	2.4333×10^4	1.2137×10^2	1.3996×10^5
	g_2	2.6968×10^5	2.6487×10^4	1.4107×10^2	
	g_3	2.3136×10^5	8.3239×10^3	5.0462×10^2	

For simplicity of analysis, the same values of initial gains are used for all different cases and the desired objective function in eqn (16) is set based upon the objective function with the initial gains. The homotopy parameter γ is chosen as 0.9, so that the desired objective function does not produce unnecessarily high values of feedback gains. Also, the constraint equation is included as a part of the overall computational process to monitor the violation of eqn (6). In this special study, the selected objective functions turn out to prevent such cases.

The feedback gains corresponding to the first mode and compensator, as in the results, show higher sensitivity or increase in values from initial values. This is due to the essential characteristics of the PFF compensators which represent second order low pass

filters. In particular with the three modes excitation, all the feedback gains are activated considerably, which is in contrast with the case where the first mode is excited and the actuator 3 makes insignificant contribution. Also, the actuator located at the root of the first structure shows higher control authority compared with the other two actuators. This can be explained by the observation that the root position of the first structural element has the highest strain energy concentration.

Furthermore, the results, by increasing $w_1 = 500$ ($w_2 = 100$), are presented in Table 2. As one could expect, the feedback gains increased compared with the case where $w_1 = 100$ ($w_2 = 100$). One important thing to be noted is the negative sign of one of the gains in Table 2. This contradicts with the original

Fig. 3. Time response results with $w_1 = 100, w_2 = 100$ (Solid line—Initial, Dotted line—Optimized).

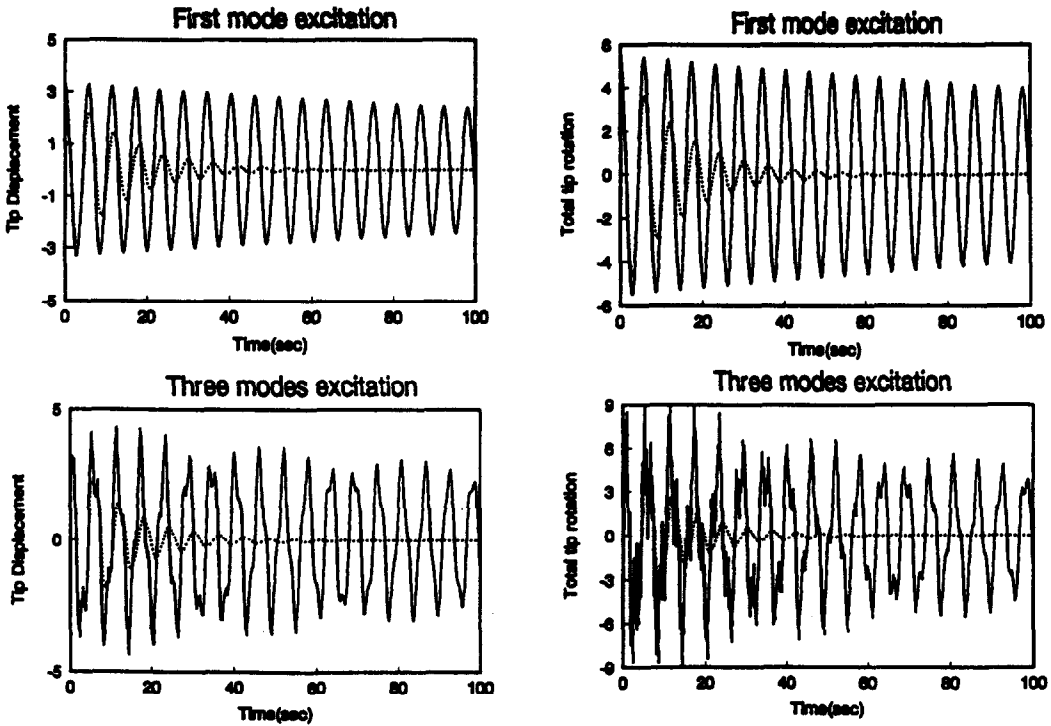


Fig. 4. Time response results with $w_1 = 500$, $w_2 = 100$ (Solid line—Initial, Dotted line—Optimized).

definition of PPF (Positive Position Feedback). It is believed that the gains are approaching the stability boundary in eqn (6) causing numerical stability problem.

Increasing the weighting factor on the total tip rotation so that $w_1 = 100$ ($w_2 = 500$) has a significant effect on the gains. The gains are biggest in this case, which implies that the rotation is more difficult to

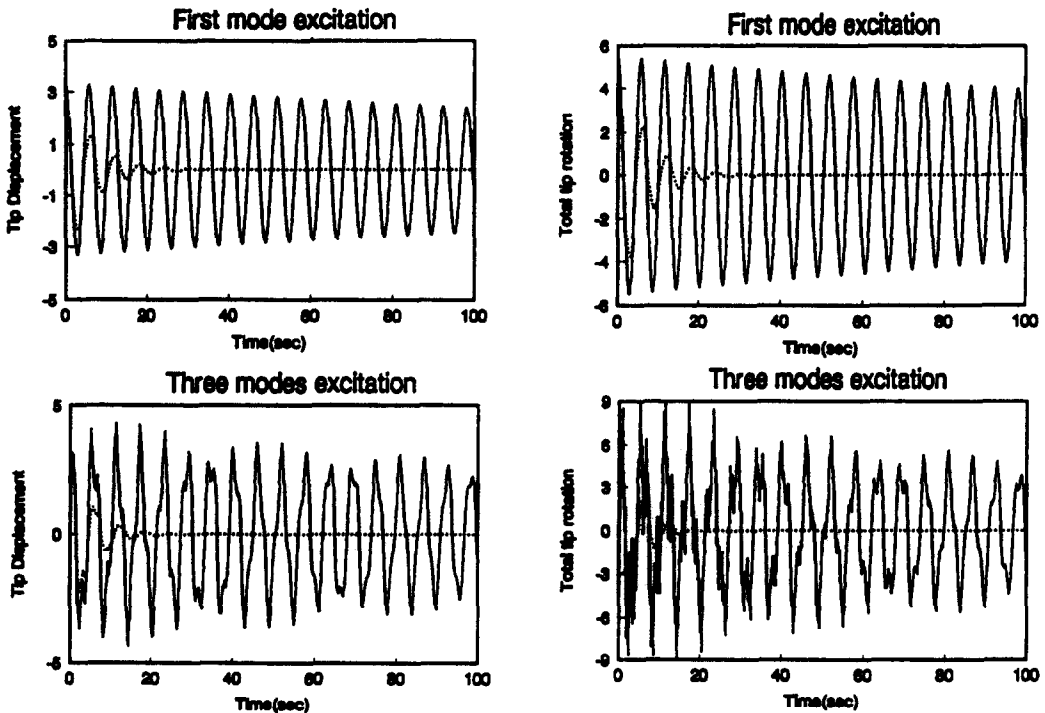


Fig. 5. Time response results with $w_1 = 100$, $w_2 = 500$ (Solid line—Initial, Dotted line—Optimized).

control than the displacement in this particular system. This confirms the visual observation of the responses of the actual system by a previous study[9].

Simulation results using the feedback gains obtained are presented in Figs. 3–5. Figure 3 presents results with $w_1 = 100$ ($w_2 = 100$), Fig. 4 with $w_1 = 500$ ($w_2 = 100$), and Fig. 5 with $w_1 = 100$ ($w_2 = 500$), respectively. The optimized gains suppressed the vibration more quickly than the initial gains. The gains obtained using $w_1 = 100$ ($w_2 = 500$) show better time responses in Fig. 5 controlling both tip displacement and rotation more effectively compared with the results in Fig. 4. The initial condition distribution has a significant effect on the optimization results, and a statistical analysis is recommended to take into account generic distribution of initial conditions.

Once again, it is not easy to make an initial guess when there are as many as nine or more feedback gains. The effect of increased weighting factor (w_2) visibly improves responses as expected from the optimization results. Our optimization approach provides us with a direct path to selecting a best set of stabilizing feedback gains for multi-input multi-output PPF compensators.

5. CONCLUSION

An optimization algorithm was successfully applied to designing an optimized compensator, so-called PPF (Positive Position Feedback) for control of flexible spacecraft model using adaptive structures. A nonlinear programming technique subject to a matrix constraint was used to minimize an objective function. The objective function can be selected based upon a specific mission requirement.

Application of the method was made for a flexible space structure model, and the results verify that the proposed method can be used to improve the performance of the conventional PPF approach.

REFERENCES

1. M. J. Balas, Trends in large space structures control theory: fondest hopes, wildest dreams. *IEEE Transactions on Automatic Control* **AC-27** (1982).
2. P. Likins, Spacecraft attitude dynamics and control—a personal perspective on early developments. *J. Guidance, Control and Dynamics* **9**, 129–134 (1986).
3. C. J. Goh and T. K. Caughey, On the stability problem caused by finite actuator dynamics in the control of large space structures. *Int. J. Control* **41**, 787–802 (1985).
4. J. L. Fanson and T. K. Caughey, Positive position feedback control for large space structures. *AIAA Journal* **28**, 717–724 (1990).
5. D. W. Rew, New feedback design methodologies for large space structures: a multi-criterion optimization approach. Ph.D. Dissertation, Virginia Polytechnic Institute and State University, Blacksburg, Virginia (1987).
6. S. Hanagud, M. W. Obal and A. J. Calise, Optimal vibration control by the use of piezoceramic sensors and actuators. *J. Guidance Control, and Dynamics* **15**, 1199–1206 (1992).
7. J. L. Junkins and Y. Kim, Minimum sensitivity design method for output feedback controllers. *Mechanics and Control of Large Flexible Structures, AIAA Progress in Astronautics and Aeronautics* **129**, 389–409 (1990).
8. H. Bang, J. L. Junkins and P. J. Fleming, Lyapunov optimal control law for flexible space structures maneuver and vibration control. *J. Astronautical Science* **41**, 91–118 (1993).
9. H. Bang and B. N. Agrawal, A generalized second order compensator for vibration control of flexible structures. *Proceedings for the 35th AIAA/ASME/ASCE/AHS/ASC Structures, Structural Dynamics, and Materials Conference*, Hilton Head, SC, 18–20 August (1994).